Published in final edited form as:
Eur J Neurosci. 2014 April ; 39(8): 1256–1267. doi:10.1111/ejn.12486.

Thrombospondins 1 and 2 are important for afferent synapse formation and function in the inner ear

Diana Mendus[1], **Srividya Sundaresan**[1], **Nicolas Grillet**[2], **Felix Wangsawihardja**[1], **Rose Leu**[1], **Ulrich Müller**[2], **Sherri M. Jones**[3], and **Mirna Mustapha**[1]

[1]Department of Otolaryngology – Head and Neck Surgery, Stanford University, Stanford, CA, USA, 94305

[2]Department of Cell Biology, The Scripps Research Institute, La Jolla, CA, USA, 92037

[3]Department of Special Education & Communication Disorders, University of Nebraska-Lincoln, Lincoln, NE, USA, 68583

Abstract

Thrombospondins (TSPs) are a family of secreted extracellular matrix proteins that have been shown to be involved in the formation of synapses in the central nervous system. In this study, we show that TSP1 and TSP2 are expressed in the cochlea, and offer the first description of their putative roles in afferent synapse development and function in the inner ear. We examined mice with deletions of TSP1, TSP2, and both (TSP1/2), for inner ear development and function. Immunostaining for synaptic markers indicated a significant decrease in the number of formed afferent synapses in the cochlea of TSP2 and TSP1/2 knockout (KO) mice at P29. In functional studies, TSP2 and TSP1/2 KO mice showed elevated auditory brainstem response (ABR) thresholds compared to wild type littermates starting at postnatal (P) day 15 with the most severe phenotype for the TSP1/2 KO mice. TSP1/2 KO mice also showed reduced wave I amplitudes of ABR and vestibular evoked potential suggesting a synaptic dysfunction in both the auditory and vestibular systems. While ABR thresholds in TSP1 KO mice were relatively unaffected at early ages, TSP1/2 double mutants exhibited the most severe phenotype among all the genotypes tested, suggesting functional redundancy between these two genes. Based on the above results, we propose that TSPs play an important role in afferent synapse development and function of the inner ear.

Keywords

mouse; hair cell; glia-like supporting cells; extracellular matrix

Correspondence should be addressed to Dr. Mirna Mustapha, Stanford University, Edwards Building, 300 Pasteur Drive, Room R111A, Stanford, CA 94305-5453. mirnam@stanford.edu.

The authors declare no competing financial interests.

Introduction

The sensory epithelium in the cochlea of the inner ear, the organ of Corti, is a precisely patterned structure consisting of the inner and outer hair cells and several types of supporting cells. In rodents, cochlear spiral ganglion neurons (SGN) projection towards hair cells starts at embryonic (E) day 12.5. The cochlea then goes through a critical process of synapse formation and refinement during the first two postnatal weeks (Rubel, 1978; Knipper et al., 1995; Appler & Goodrich, 2011) with the onset of hearing occurring by postnatal (P) day 12–14. Any defect at this stage of maturation can result in a dysfunctional hearing organ and is one of the causes of auditory neuropathy or synaptopathy (Starr *et al*., 2008; Santarelli, 2010).

Recent studies reveal important roles for extracellular matrix molecules such as thrombospondins (TSPs) in promoting synapse formation during development in the central nervous system (CNS) and in repairing synaptic connection after stroke (Christopherson *et al*., 2005; Liauw *et al*., 2008; Xu *et al*., 2010). TSPs are a family of multifunctional proteins that are being increasingly recognized for a variety of important physiological roles in development and disease (Tooney *et al*., 1998; Swinnen *et al*., 2009; Kim *et al*., 2012; Tran *et al*., 2012) in many systems including cardiovascular and CNS. Their physiological actions are mediated by regulating cell-cell and cell-matrix interactions through partnering with an array of membrane receptors, other extracellular matrix proteins and cytokines. TSPs and are secreted by astrocytes in the CNS (Bornstein, 2000; Bentley & Adams, 2010; Risher & Eroglu, 2012) and can be structurally divided into two groups: Group A, contains the highly homologous TSP1 and TSP2 proteins and Group B, consists of TSPs 3, 4 and 5 (Adams & Lawler, 2004; Carlson et al., 2008). Mice deficient in TSP1 and TSP2 or both can develop abnormalities in lungs, muscles, bones, heart and brain (O'Shea *et al*., 1990; Kyriakides *et al*., 1998; Lawler *et al*., 1998; Swinnen *et al*., 2009). In a purified retinal ganglion cell system, TSP1 and TSP2 were shown to be necessary and sufficient signals coming from astrocytes to stimulate excitatory synaptogenesis (Christopherson *et al*., 2005). Intriguingly, TSP2 mRNA was upregulated in a thyroid-deficient mouse model with defective synaptic maturation, compared to wild type (WT) controls (Sendin *et al*., 2007; and our data, unpublished). Based on the above findings, we hypothesized that TSPs may be involved in synapse formation in the cochlea.

In this study, we examined whether TSPs play a role in cochlear and vestibular afferent synapse formation and function using mice with targeted deletions of either one or more than one TSP gene. TSP3, TSP4 and TSP5 KO mice do not show an auditory phenotype. TSP2 and TSP1/2 KO mice have reduced number of afferent ribbon synapses, and varying degrees of impaired auditory and vestibular function compared to WT littermates, with TSP1/2 KOs showing the most severe phenotype. In summary, these findings indicate that TSP1 and TSP2 act redundantly to insure normal synapse formation and function of the inner ear.

Materials and Methods

Animals

Mice of either sex lacking TSP1 (TSP1 KO) (Lawler *et al*., 1998), TSP2 (TSP2 KO) (Kyriakides *et al*., 1998) or double mutants (TSP1/2 KO) (Agah *et al*., 2002) and their littermate WT controls were used for experiments. These mice are on an FVB/NJ genetic background. At least three animals per genotype per experiment were used and experiments were repeated two to three times for validation. All experiments were completed with national animal care guidelines and were approved by the Stanford University Administrative Panel on Laboratory Animal Care.

RNA extraction and quantitative RT-PCR (qPCR)

RNA was extracted from whole cochlea dissected from WT FVB mice at the postnatal day(s): P0 (n=4), P6 (n=3), P10 (n=4), P15 (n=5) and P29 (n=5) for TSP2 and additionally at P60 (n=3), P180 (n=5) for TSP1 or whole vestibular organ dissected from WT FVB mice at the postnatal day(s): P6 (n=6), P10 (n=4), P16 (n=7), P30 (n=4) for all genes tested using an RNAqueous-Micro Kit from Ambion according to the protocol of the manufacturer. Extracted RNA was converted to cDNA using a High Capacity RNA to cDNA kit (Applied Biosystems). This cDNA was used in amplified in PCR assays with Taqman (Applied Biosystems) proprietary probes and primers for TSP1 (assay ID Mm01335418_m1) and TSP2 (assay ID Mm01279240_m1). GAPDH (assay ID Mm03302249_g1) was used as the internal standard. All Taqman qPCR assays were performed on a BIO-RAD CFX96™ Real-Time System with accompanying software for data analysis. Data are shown as relative normalized expression of the gene of interest with respect to the internal standard, GAPDH. Error bars represent standard error of the mean (SEM).

In situ hybridization

TSP-specific *in situ* probes were generated from 5′ part of the full length cDNA. Fragments were subcloned from IMAGE clones (Openbiosystem ID 64050917 and Openbiosystem ID 30062369, respectively) into pGEM-T vector (Promega) using the following primers: TSP1: ATGGAGCTCCTGCGGGGACTA and ATCAGGAACTGTGGCGTTGGAGCA [1098bp]; TSP2: ATGCTCTGGGCACTGGCCCTGCT and TTCCACAAAAGATGGGTTGGCACAA [1101bp]. *In situ* hybridization was carried out as previously described (Schwander *et al*., 2007).

Immunohistochemistry

Inner ears were dissected into cold phosphate buffered saline (PBS) and after opening oval, round windows and the bone on the cochlear apex, cochleae were perfused with 4% paraformaldehyde in PBS and were left in fixative solution for additional 10 minutes. Samples were washed in PBS for 10 minutes and then blocked in PBS containing 0.5% Triton X-100 plus 5% bovine serum albumin for 30 minutes at room temperature. Same blocking buffer was used for diluting antibodies. Primary antibodies were incubated in 4°C for 36 hours followed by three washes in 0.1% PBS-Tween. Secondary antibodies were added for 1 hour at room temperature, followed by three washes in 0.1%PBS-Tween. The

following primary antibodies were used: goat anti-CtBP2 (1:200, Santa Cruz Biotechnology) for RIBEYE, rabbit anti-Glutamate Receptor 2&3 (1:100 dilution, Millipore Biosciences Research Reagents), rabbit anti-HOMER1 (1:200 dilution, Synaptic System), rabbit anti-SHANK1 (1:200 dilution, Neuromics). Secondary antibodies used were Alexa Fluor 488-conjugated anti-goat, Alexa Fluor 546-conjugated anti-rabbit (1:500 dilution, Invitrogen). After immunostaining, cochleae were decalcified in 10% EDTA for 1 hour at room temperature and further fixed by immersion in 4% paraformaldehyde in PBS for 15 minutes. Cochleae or vestibular utricles were washed in PBS and mounted on slides in ProLong (Invitrogen) anti-fading media.

Confocal analysis of synapse number

Images of immunostained organ of Corti or vestibular utricle were collected on Zeiss AxioVert confocal inverted microscope. Optical sections were line and frame averaged and collected at 0.3 um intervals with a1024×1024 raster. Detector gain and excitation thresholds were adjusted per tissue to cover the same range of pixel values while the pinhole was calibrated for the WT animal tissues and kept constant for all samples. Cochlear frequency map (Muller *et al*., 2005) was estimated for every sample to localize hair cells from different frequency regions. Cochlear z-stacks from a selected frequency region were taken for each sample. Each stack contained the entire synaptic pole of 15–20 inner hair cells. Synapses were automatically counted through the series of optical sections using the Volocity 3D Image Analysis Software. To confirm the accuracy of the counts, z-stacks were manually quantified for synapse number by projecting a series of optical sections and counting synaptic puncta in each projection volume. On average, one stack per cochlear/vestibular region was obtained from six different animals. For tissues double-labeled with pre- and postsynaptic markers, a total of at least 4 scans per genotype at P29 were analyzed using automatic counts in Volocity 3D Image Analysis Software, and confirmed manually as well. Statistical analyses were performed using an SPSS (Statistics Premium Grad Pack, Version 20.0 for Mac OS, IBM Corporation) software package. One-way analysis of variance (ANOVA) of synaptic marker counts as dependent variable and genotypes (WT, TSP1, TSP2 and TSP1/2) as factor, followed by Scheffe's post-hoc test, was performed for RIBEYE, SHANK1 and colocalized (synaptic) puncta. $P < 0.05$ was considered statistically significant.

Auditory Brainstem Responses (ABR)

ABR recordings were conducted in a sound-attenuating room at Auditory Core for Department of Otolaryngology, Stanford University. Mice were weighed and anesthetized with ketamine (100 mg/kg) and xylazine (10 mg/kg) was injected intraperitoneally. Core body temperature was kept at 37.0 C for all recordings using a homeothermic heating pad (FHC). Stimulus presentation, ABR acquisition, equipment control and data management were coordinated using the computerized Intelligent Hearing System (HIS, Miami, FL). A high frequency transducer was coupled with the IHS system to generate specific acoustic stimuli. Acoustic stimuli were delivered to the animal's ear canals via plastic tubes channeled to the speaker at 8, 16 and 32 kHz. ABRs were recorded via sub dermal needle electrodes inserted at the vertex (active electrode), behind the left pinna (reference electrode), and in the left leg (ground electrode). Electrophysiological activity was

amplified, filtered and averaged. Sound levels were incremented in 5 dB steps from 10–20 dB below threshold to 80 dB (for 8 and 16 kHz) or 100 dB (for 32 kHz). Threshold for ABR was defined as the lowest stimulus level at which replicable waves I and V could be identified in the response waveform. The amplitude analysis was done by peak-to-peak measurement of the ABR waveform and latency was calculated as time from stimulus onset until the respective peak. ABR waveform amplitude and latency analysis was performed for 16 kHz at 65 dB. Statistical analyses were performed using an SPSS software package. One-way ANOVA of either amplitude or latency as dependent variables and genotypes (WT, TSP1 K/O, TSP2 K/O, TSP1/2 KO) as factor, followed by Scheffe's post hoc test, was performed at specific ages (1 month or 3 months). Two-way ANOVA of the ABR data was performed with ABR thresholds as dependent variable and genotypes (WT, TSP1 K/O, TSP2 K/O, TSP1/2 KO) and age as independent factors. Based on significant main effects and interactions from this statistical test, planned comparisons were performed using a one-way ANOVA with ABR thresholds as dependent variable, followed by Scheffe's post hoc test to identify differences between genotypes, or across the ages tested, at a given frequency (8, 16 or 32 kHz). In all statistical tests, $P < 0.05$ was considered statistically significant.

Vestibular evoked potentials (VsEPs)

Gravity receptor neural function was assessed with linear VsEPs. VsEPs were recorded from mice of either sex at 1.5 months of age from four genotypes. Recording method was similar to Mock *et al*. (2011). In short, mice were weighed and anesthetized with ketamine and xylazine, similarly as for ABR recordings. Core body temperature was maintained at 37.0°C. The active electrode was placed subcutaneously at the midline just posterior to the lambdoidal suture; the reference electrode was placed behind the right pinna and the ground at the right leg. Mice were positioned supine; a non-invasive head clip was used to secure the head to a mechanical shaker for delivery of the vestibular stimuli. Stimuli were linear acceleration pulses, 2 ms duration, and 17 pulses per second, applied to the cranium in the naso-occipital axis. Stimulus amplitude ranged from +6 to −18 dB relative to 1.0 g/ms (1g = 9.8 m/s^2) in 3 dB steps. Beginning at stimulus onset, electrophysiological activity was amplified, filtered, and digitized. A broadband masker was used to verify the absence of auditory responses. The first positive and negative response peaks were scored for VsEPs as this response peak is generated by the peripheral eighth nerve. Thresholds (in dB), first wave amplitude (in microvolts – μV), peak latency (in milliseconds - ms) were quantified and compared across genotypes. Statistical analysis was performed using a one-way ANOVA of VsEP latency or amplitude as dependent variables and genotypes (WT, TSP1 K/O, TSP2 K/O, TSP1/2 KO) as factor, followed by Scheffe's post-hoc test. $P < 0.05$ was considered statistically significant.

Results

Expression of TSP1 and TSP2

To determine the relative expression levels of TSP1 and TSP2 transcripts in the mouse cochlea, we performed quantitative RT-PCR (qPCR) with specific, validated primers sets on RNA extracted from cochlea of wild type FVB/NJ mice at different developmental ages. We found that mRNA levels for TSP1 were substantially higher between P0 and P29 compared

to P48 and P60 (Fig. 1A). At P180, TSP1 expression levels remained low. TSP2 was highly expressed at birth and decreased thereafter (Fig. 1B). By P29, TSP2 expression was almost undetectable in the cochlea. Elevated levels of mRNAs for TSPs 3, 4 and 5 were also seen between P0 and P29 (data not shown).

In order to more precisely localize TSP expression in the cochlea, we performed *in situ* hybridization at late embryonic (E) and early postnatal (P) periods, when afferent synaptogenesis is ongoing in the cochlea (Sobkowicz *et al*., 1982; Appler & Goodrich, 2011). At E17 and P1, TSP1 expression was observed in the supporting cells (SCs) of the organ of Corti, surrounding inner and outer hair cells including the inner sulcus, phalangeal, pillar and Dieters cells (Fig. 1C, E, E′). At P5, TSP1 expression was restricted to pillar cells and to inner sulcus cells (Fig. 1E″) of the sensory epithelium. TSP1 expression was also widespread in the cochlear bony tissue. No signal was observed with control sense probe (Fig. 1D, F–F″). Expression of otoferlin (OTOF) is shown as a positive control that marks the IHCs and OHCs (Fig. G–G″). We speculated that TSP2 would also be expressed by the supporting cells of the cochlea, but *in situ* hybridization with multiple TSP2 probes did not yield convincing results for cochlear tissue at the same ages as described for TSP1. The above results show that TSP1 and TSP2 are both expressed in the cochlea and are developmentally regulated. We next examined whether these molecules are involved in cochlear synaptogenesis.

Cochlear synaptogenesis in TSP mutants versus control WT mice

Initial examination of gross cochlear morphology using plastic embedded sections did not show significant differences between the wild type and the different mutant strains (data not shown). However, to examine whether TSP1 and TSP2 may cause more subtle changes, as would be expected with a synaptogenic role, we looked at the number of synapses in the mature organ of Corti at P29 in WT and TSP1, TSP2 and TSP1/2 KO mice. We examined pre- and postsynaptic afferent markers at the IHC by immunostaining. We focused on the 16 kHz region that has the highest synaptic density and hearing sensitivity in mice (Liu & Davis, 2007; Meyer *et al*., 2009). Confocal images of whole mount prepared cochleae were reconstructed in z-stacks using Volocity 3D Image Analysis software to count numbers of synaptic puncta. First, we looked at the presynaptic marker RIBEYE that is a main protein of synaptic ribbons (Schmitz *et al*., 2000). A one-way ANOVA of RIBEYE marker counts as dependent variable and genotypes as independent factor was significant ($F_{3,40} = 8.001$, $P = 0.000$). Scheffe's post hoc test showed that there was a significant reduction in the number of RIBEYE positive puncta in TSP2 ($P = 0.002$) and TSP1/2 ($P = 0.007$) mutants as compared to WT mice (Fig. 2A, B). To examine the postsynaptic side, we labeled the AMPA receptor GLUR2/3 (Tanabe *et al*., 1992; Nakanishi, 1994; Puel, 1995) and scaffolding proteins of postsynaptic density, HOMER1 (Xiao *et al*., 1998, 2000) and SHANK1 (Naisbitt *et al*., 1999; Tu *et al*., 1999) (data shown for SHANK1 only). Using the same confocal approach, counts at the 16 kHz region indicated no significant differences (one way ANOVA, $F_{3,25} = 1.662$, $P = 0.201$) in SHANK1 staining between WT and TSP single and double KOs (Fig. 2C, D).

To verify that stained puncta correspond to synapses (as defined by juxtaposition of pre- and postsynaptic terminals and henceforth referred to as “synapses”), we double labeled cochlear whole mount preparations of WT and TSP KOs using antibodies to RIBEYE and SHANK1 (Fig. 2E, F). There was a 16% decrease in synapses in TSP1 KOs (8.0 per IHC as compared to 8.8 in WT), 25% decrease in TSP2 KOs (6.4 per IHC as compared to 8.8 in WT) and 43% reduction in TSP1/2 double KOs (3.7 per IHC as compared to 8.8 in WT) (Fig. 2E, F). There was more orphan RIBEYE staining in TSP1/2 mutants but not as much orphan SHANK1 staining. Since the above results showed that IHCs of TSP1, TSP2, and TSP1/2 KOs have reduced number of synapses, we next examined the effect of these synaptic deficits on auditory function.

Assessment of ABR thresholds in TSP1 and TSP2 mutant mice

To determine the functional consequences of loss of TSP1 and/or TSP2 for hearing function, we performed neurophysiological ABR tests in all three types of TSP mutant mice at different ages starting from P15 and ending by 18 months of age. WT littermates on the same FVB/NJ background were used as controls. To determine auditory thresholds, ABR measurements were obtained for three frequencies representing each turn of the cochlea: 8 kHz for apical turn, 16 kHz for middle turn and 32 kHz to assess function at the base of the cochlea. Mice are born deaf with onset of hearing around P12–P14. Therefore, we started testing for ABR thresholds at P15 to assess cochlear function as soon as possible after the onset of hearing. We measured hearing again at 1 month, 3 months, 6 months (data not shown), 12 months and 18 months of age. For statistical analysis, a two-way ANOVA of the ABR data was performed with ABR thresholds as dependent variable and genotypes (WT, TSP1 K/O, TSP2 K/O, TSP1/2 KO) and age (P15, 1, 3, 6, 12, and 18 months) as independent factors. This analysis showed significant main effect of genotype by age interaction ($F_{15,193} = 8.668$, $P = 0.000$). Planned comparisons were performed using a one-way ANOVA with ABR thresholds as dependent variable and either age or genotype as independent factors. This analysis was followed by Scheffe’s post hoc test to identify differences between genotypes, or across the ages tested, at a given frequency (8, 16 or 32 kHz). TSP1/2 mutants exhibited elevated thresholds at all frequencies tested starting as early as P15 (Fig. 3A, B, C). TSP2 mutants at P15 had elevation at 8 and 32 kHz regions. (Fig. 3A, C). TSP1 mutants had normal hearing thresholds at all frequencies tested (Fig. 3A, B, C) at P15. There were no further changes in ABR thresholds for the different mutant mice at 1 month, 3 months (Fig. 3A, B, C) and 6 months (not shown) of age. However, at 12 months of age, there were greater threshold shifts at all frequencies tested in TSP2 and TSP1/2 mutants (Fig. 3). At 12 months of age, TSP1 mutants show a significant ($P = 0.000$) threshold elevation only at 32 kHz. Beyond 12 months, all genotypes experience profound threshold elevation at 32 kHz due to ageing, and therefore no comparisons were made beyond 12 months for this frequency. The stronger threshold shifts in TSP1/2 KOs versus single KO animals suggests functional compensation between TSP1 and 2 genes. ABRs of 1 month-old single TSP3, 4 and 5 mutants were normal compared to their WT controls (data not shown). However we cannot rule out if any of these mutants might have hearing phenotype when in combination of double or triple TSP3, 4 and 5 KOs. The above results show that the TSP2 KOs had a more severe phenotype than TSP1 KOs, and that the TSP1/2 double KOs had the strongest hearing defect among the genotypes tested. To assess the

relative contribution of TSP1 and TSP2 to cochlear neuronal activity we next examined the waves of ABR in these mutants.

Analysis of the first ABR wave amplitude and latency

It has been shown that the ABR threshold does not always reflect subtle phenotypes in the number of neurons that are firing (Liberman, 1982; Kugawa & Liberman, 2009). Therefore, we further analyzed the ABR data to identify possible changes in peak amplitude or latency. We analyzed ABR responses at 65 dB SPL, which is at least 30 dB above the hearing threshold in mice and provides a robust measure of sound-evoked neuronal activity (Fig. 4A, B). Furthermore, 16 kHz represents the most sensitive hearing region in mice. A one-way ANOVA for amplitude data as dependent variable and genotypes as independent factors showed significant differences between groups ($F_{3,33} = 4.789$, $P = 0.007$). Scheffe's post hoc test showed a significant ($P = 0.026$) reduction in the wave I response amplitude (shown as P1 - N1 values, where P1 is the first robust positive peak in the ABR trace and N1 is the negative component following P1) TSP1/2 KOs as compared to WT starting from 1 month of age (Fig. 4A, C). TSP2 KOs showed no significant wave I amplitude changes at 1 month or at 3 months (Fig. 4C, D). Likewise, TSP1 KOs did not show significant changes in wave I amplitudes at 1 month or 3 months (Fig. 4C, D). Peak latency of the wave I ABR was significantly prolonged in the TSP1/2 KOs at 1 month ($P = 0.031$) and 3 ($P = 0.001$) months of age compared to WT. Latencies for TSP1 and TSP2 KOs were similar to WT at both tested ages (Fig. 4E, F). Analysis of the wave I ABR peak at 8 kHz also showed significant differences in the amplitude and latency in TSP1/2 KOs versus WT at 1 month of age (data not shown). Analysis of the wave II ABR peak performed for 16 kHz at the 65 dB SPL at this age showed results similar to that of the wave I ABR peak (data not shown). Amplitudes of the wave I ABR peaks in TSP3, 4 and 5 mutants at 16 kHz and 65 dB SPL were comparable to their WT controls (data not shown). The above results show that amplitude and latencies of the TSP1/2 KOs were the most affected, starting at 1 month of age when the other KOs were similar to WT.

Characterization of vestibular function in the TSP mutants

As many genes that have been shown to be important for cochlear function were also reported to be involved in vestibular function (Moller, 2002; Nandi & Luxon, 2008), we investigated whether TSP1 and 2 are expressed in the vestibular system and if they play a role in the function of the inner ear gravity receptor organs (Eatock & Songer, 2011). qPCR analysis of vestibular tissue showed expression profiles for TSP1 and TSP2 genes that were similar to cochlear tissue (Fig. 5A, B). Highest levels for both genes were seen at P6, the earliest age tested. TSP1 expression remained at the same level from P6 to P16 and then declined but TSP2 expression declined soon after P6. To more precisely localize TSP expression in the vestibular system, we performed *in situ* hybridization on the neonatal utricle at P1 (Fig. 5C). Strong TSP1 mRNA expression was seen at the apical side of the utricle sensory epithelium (Fig 5C–C′). We were again unable to specifically localize TSP2 mRNA by this technique. No signal was observed with control sense probe (Fig. 5D–D′). Expression of OTOF is shown as a positive control that marks the type I and type II hair cells (Fig. 5E–E′). Immunostaining for pre- and postsynaptic markers, RIBEYE and SHANK1, respectively, on the sensory epithelium of the P29 mouse utricle showed reduced

($P = 0.001$) synaptic ribbon staining in TSP1/2 KOs as detected with a RIBEYE antibody (Fig. 6A, D, G). SHANK1 staining appeared similar between WT and TSP1/2 KOs (Fig. 6B, E, H). The number of colocalized synaptic puncta was also significantly ($P = 0.000$) reduced in TSP1/2 mutants compared to WT controls (Fig. 6I). We also examined cryosections of the vestibular utricle for these markers with similar results (data not shown). To assess gravity receptor function, we measured VsEP responses in 1.5 months-old WT and mutant mice. One-way ANOVA of VsEP data showed significant differences among genotypes for VsEP thresholds ($P = 0.020$) and wave I (P1 - N1) amplitudes ($P = 0.040$). Post hoc comparisons revealed no differences in VsEP thresholds between TSP1 mutants as compared to WT mice at this age. However, TSP2 ($P = 0.020$) and TSP1/2 double mutants ($P = 0.010$) had significantly elevated thresholds as compared to WT animals (Fig. 7B). Amplitudes at +6 dB for the wave I response peak were also significantly reduced for TSP1/2 mutants as compared to WT controls ($P = 0.011$) (Fig. 7A, C). Analysis of the wave I peak latencies at +6 dB did not show significant differences among genotypes (Fig. 7D). Vestibular behavioral dysfunction, as measured by a swimming test, did not reveal obvious differences between the various mutant and wild type strains (data not shown). Overall, these results show that while the vestibular phenotype is somewhat subtle, TSP2 and TSP1/2 mutants have reduced sensitivity of the peripheral gravity receptor organs.

Discussion

Data presented in this study show for the first time that TSPs 1 and 2 play important synaptogenic roles in the cochlear and vestibular organs. Furthermore, the physiology experiments demonstrate that synaptic defects in mice deficient in TSPs 1 and 2 or both, could at least partially account for the hearing loss seen in these mice. The more severe phenotype of the double KOs over the single TSP1 or TSP2 KOs points to a redundancy in this system. TSP2 appears to compensate somewhat for the absence of TSP1, whereas the reverse effect of TSP1 compensating for lack of TSP2 does not appear to be robust. These studies are novel in their scope and the first demonstration to date of the effect of synaptogenic molecules of the extracellular matrix in the development and function of cochlear and vestibular systems.

TSP expression in the inner ear

The *in situ* hybridization analysis for TSP1 (Fig. 1) showed early expression in the SCs such as the inner phalangeal, pillar and Dieter's cells up to P5. This result suggests that SCs of the inner ear may play a similar role to glial cells in the brain in providing critical factors for synapse formation and maintenance (Pirvola *et al*., 1994; Ullian *et al*., 2001; Dityatev *et al*., 2006; Sugawara *et al*., 2007; Gomez-Casati *et al*, 2010; Tritsch & Bergles, 2010; Zuccotti *et al*., 2012; Clarke & Barres, 2013). Restriction of TSP1 expression to a small subset of SCs at P5, from initial widespread expression in the cochlea, also points to diversity in the functions of the various types of SCs in this tissue (Rio *et al*., 2000; Monzack & Cunninham, 2013; Wan *et al*., 2013). Our qPCR studies showed high expression of TSP1 and TSP2 during the first postnatal week in the mouse cochlea. TSP2 expression decreased by P10, coordinating with a reported decrease in synaptogenesis in the cochlea (Huang *et al*., 2007; Huang *et al*., 2012). TSP1 expression subsequently decreased at P60, by which

time the cochlea is fully mature. Interestingly, while the expression of TSP2 is practically undetectable by P29, expression of TSP1 did not entirely disappear at later ages suggesting a more sustained role for these genes in the cochlea. These spatial and temporal gene expression data strengthen the notion that SCs are involved in providing critical factors, such as TSPs, required for afferent synapse formation (Christopherson *et al*., 2005).

Involvement of TSPs in cochlear synaptogenesis

We see a significant reduction in staining with the presynaptic ribbon marker RIBEYE but not in the postsynaptic marker SHANK1 in the cochlea of TSP mutants by P29. This observation is in agreement with previous data showing that addition of TSP1 or TSP2 alone to the cell cultured medium mainly acted on the presynaptic side leading to the formation of silent synapses and did not appear to be involved in the maturation of postsynaptic densities (Christopherson *et al*., 2005; Allen *et al*., 2012). TSP2 and TSP1/2 double mutants exhibited significant reduction in colocalized synaptic puncta supporting the important role for TSPs in cochlear synaptogenesis. Reduction in presynaptic ribbon numbers in these mutants would result in decreased number of ribbons available to form functioning synapses with postsynaptic structures. In turn, this decrease in the number of functioning synapses would result in fewer synapses firing in response to a given stimulus compared to WT controls, as reflected by the ABR data.

Since TSP1 and TSP2 are highly homologous genes, one could speculate on a certain degree of redundancy in this system as is indeed suggested by the severe phenotype in the TSP1/2 double mutants compared to TSP2 KOs. Greater loss of synaptic numbers in TSP2 KOs as compared to TSP1 mutants also indicates that TSP2 is able to partially compensate for TSP1 and that possibly the role of TSP2 is more crucial in establishing the neuronal network in the inner ear.

Contribution of TSPs to cochlear physiology

A single SGN forms a synapse with single IHC (Spoendlin, 1969; Liberman, 1980; Liberman *et al*., 1990; Raphael & Altschuler, 2003) and SGNs that contact a single IHC can be divided into at least two groups based on the rate of firing: high spontaneous rate (SR) and low SR fibers (Liberman, 1982; Liberman *et al*., 2011; Taberner & Liberman, 2005; Furman *et al*., 2013). Measurements of ABR thresholds in TSP mutants and comparison to WT controls allowed us to study general function of the cochlea. ABR threshold responses compared across the different mutants and throughout the hearing ages of a mouse (P15-P540 or two weeks and 18 months of age) showed varying degrees of hearing loss in the KO mice as compared to WT controls. The stronger phenotype in double mutants TSP1/2 suggests that TSP2 is able to compensate for the loss of TSP1 at younger ages. However, as the TSP1 mutants age, elevated ABR thresholds were seen at all frequencies by 12 months of age compared to WT controls suggesting that lack of TSP1 may affect long term maintenance of hearing. This effect on long term maintenance is likely to be more due to the initial effects of TSP1 during development rather than at later ages since we see very low levels of TSP1 mRNA beyond P29. Therefore, TSP1 may be important in establishing those elements of a stable neuronal network in the developing cochlea that are needed to sustain auditory function over the course of a rodent’s hearing lifetime. The observation of an early

threshold shift at P15 at the 32 kHz frequency in TSP2 KOs suggests that TSP2 may play an important role in the onset of hearing in the high frequency range. It is not surprising to see mutations in a synapse-related protein causing progressive high frequency hearing impairment since it was previously described in patients and mice with Vglut3 mutations (Ruel *et al*., 2008). In addition, gross morphology and staining for prestin and myosin 7 in the mutant OHCs appeared to be normal when compared to WT controls (data not shown).

The results from synapse counting and ABR threshold measurements allow us to draw a connection from the establishment of functional synapses early in development by a network of genes (such as TSPs) to the onset and maintenance of hearing function. A lack or defect in one of these genes may not manifest in hearing impairment (such as in the TSP1 KO) since synaptic defects can be very subtle, and also due to inherent redundancy in the system where another molecule with similar structure can substitute for the missing factor. However, when more than one such gene is affected (as in the TSP1/2 KO), a more obvious hearing phenotype becomes apparent. Furthermore, the lack of normal synapse patterning during development may impact the ability of an affected individual to retain normal hearing over a lifetime that may include challenges in the form of environmental insults, ageing or disease.

To better estimate the number of neurons firing in these animals, we measured the amplitude and latency of the ABR wave I and picked a frequency (16 kHz) where TSP1 and TSP2 mutants exhibited no elevation in threshold. We hypothesized that amplitude loss in TSP mutants would correlate with loss of synaptic function. Analysis of the first peak of ABRs in TSP mutants was in agreement with histological data that showed reduction in juxtaposed pre- and postsynaptic markers. Physiologically, this result correlated with the most significant reduction in first peak amplitude seen in TSP1/2 double KOs, followed by TSP2 mutants. These data suggest that TSP2 may functionally compensate for the absence of TSP1, at least initially.

Contribution of TSPs to vestibular physiology

We saw reduced density of synaptic ribbons in the vestibular organs of TSP1/2KOs, further supporting the idea that lack of TSPs results in loss of synapses. Since a lack of genes affecting synapse function may not necessarily cause a visible behavioral defect, such as circling, we used VsEPs as a measure of vestibular neural activity (Jones *et al*., 2002). VsEP thresholds were elevated in both TSP2 and TSP1/2 mutants compared to controls, similar to the auditory phenotypes in these animals. The onset of the compound action potential was not altered in TSP mutants, although such a functional defect was observed in the cochlea through the prolonged latencies in TSP1/2 KOs.

In summary, this study shows for the first time that TSPs that are expressed in the inner ear during the critical window of postnatal synaptogenesis play an important role in establishing connectivity between IHCs and SGNs. The data presented above show that a lack of TSPs leads to defective synapse formation in the inner ear. This synaptic defect in turn leads to fewer functional synapses responding to a given stimulus and impaired auditory and vestibular function, especially in mice that are deficient in both TSP1 and TSP2. These results also indicate that while TSP2 plays a more important role in the development of

auditory function and is able to mostly compensate for the lack of TSP1, there could be some redundancy in the system. This study shows that the components of the extracellular matrix, such as TSPs, play an important role in afferent synapse development and functional maturation in the inner ear and are candidates for screening in patients with various forms of inner ear dysfunction.

Acknowledgments

This work was supported by research and core grants from the National Institute in Deafness and other Communicative Disorders: RO1 DC09590 (Dr. Mirna Mustapha), P30 DC010363 (Dr. Stefan Heller, Stanford University), R01 DC006443 (Dr. Sherri Jones), as well as Child Health Research Institute, Lucile Packard Foundation for Children's Health, Stanford CTSA Grant: UL1TR000093 (Dr. Diana Mendus). The authors thank Drs. Ben Barres and Nicola Allen for providing TSP1/2 KOs and for discussions; Drs. Cagla Eroglu, Jacqueline Hecht, Karen Posey for providing TSP4 KO, TSP3 KO and TSP5 KO mice respectively; Patrick Raphael for assistance with vestibular test; Dr. Anthony Ricci for critical discussions; Dr. Srikantan Nagarajan for guidance with statistical analysis of the data and Dr. Simon S. Gao for helpful comments on this manuscript.

Abbreviations

aBR	auditory brainstem response
CNS	central nervous system
E	embryonic
SGN	spiral ganglion neuron
HC	hair cell
IHC	inner hair cell
KO	knockout
OTOF	otoferlin
P	postnatal
qPCR	quantitative RT-PCR
SGN	spiral ganglion neuron
SC	supporting cell
SEM	standard error of mean
SR	spontaneous rate
TSP	thrombospondin
WT	wild type
VsEP	vestibular evoked potential

References

Adams JC, Lawler J. The thrombospondins. Int J Biochem Cell Biol. 2004; 36:961–968. [PubMed: 15094109]

Agah A, Kyriakides TR, Lawler J, Bornstein P. The lack of thrombospondin-1 (TSP1) dictates the course of wound healing in double-TSP1/TSP2-null mice. Am J Pathol. 2002; 161:831–839. [PubMed: 12213711]

Allen NJ, Bennett ML, Foo LC, Wang GX, Chakraborty C, Smith SJ, Barres BA. Astrocyte glypicans 4 and 6 promote formation of excitatory synapses via GluA1 AMPA receptors. Nature. 2012; 486:410–414. [PubMed: 22722203]

Appler JM, Goodrich LV. Connecting the ear to the brain: Molecular mechanisms of auditory circuit assembly. Prog Neurobiol. 2011; 93:488–508. [PubMed: 21232575]

Bentley AA, Adams JC. The evolution of thrombospondins and their ligand-binding activities. Mol Biol Evol. 2010; 27:2187–2197. [PubMed: 20427418]

Bornstein P. Matricellular proteins: an overview. Matrix Biol. 2000; 19:555–556. [PubMed: 11102745]

Carlson CB, Lawler J, Mosher DF. Structures of thrombospondins. Cell Mol Life Sci. 2008; 65:672–686. [PubMed: 18193164]

Christopherson KS, Ullian EM, Stokes CC, Mullowney CE, Hell JW, Agah A, Lawler J, Mosher DF, Bornstein P, Barres BA. Thrombospondins are astrocyte-secreted proteins that promote CNS synaptogenesis. Cell. 2005; 120:421–433. [PubMed: 15707899]

Clarke LE, Barres BA. Emerging roles of astrocytes in neural circuit development. Nat Rev Neurosci. 2013; 14:311–321. [PubMed: 23595014]

Dityatev A, Frischknecht R, Seidenbecher CI. Extracellular matrix and synaptic functions. Results Probl Cell Differ. 2006; 43:69–97. [PubMed: 17068968]

Eatock RA, Songer JE. Vestibular hair cells and afferents: two channels for head motion signals. Annu Rev Neurosci. 2011; 34:501–534. [PubMed: 21469959]

Furman AC, Kujawa SG, Liberman MC. Noise-induced cochlear neuropathy is selective for fibers with low spontaneous rates. J Neurophysiol. 2013

Gomez-Casati ME, Murtie JC, Rio C, Stankovic K, Liberman MC, Corfas G. Nonneuronal cells regulate synapse formation in the vestibular sensory epithelium via erbB-dependent BDNF expression. Proc Natl Acad Sci U S A. 2010; 107:17005–17010. [PubMed: 20837532]

Huang LC, Barclay M, Lee K, Peter S, Housley GD, Thorne PR, Montgomery JM. Synaptic profiles during neurite extension, refinement and retraction in the developing cochlea. Neural Dev. 2012; 7:38. [PubMed: 23217150]

Huang S, Chen XH, Payne JR, Pennell DJ, Gohlke P, Smith MJ, Day IN, Montgomery HE, Gaunt TR. Haplotype of growth hormone and angiotensin I-converting enzyme genes, serum angiotensin I-converting enzyme and ventricular growth: pathway inference in pharmacogenetics. Pharmacogenet Genomics. 2007; 17:291–294. [PubMed: 17496728]

Jones SM, Subramanian G, Avniel W, Guo Y, Burkard RF, Jones TA. Stimulus and recording variables and their effects on mammalian vestibular evoked potentials. J Neurosci Methods. 2002; 118:23–31. [PubMed: 12191754]

Kim DS, Li KW, Boroujerdi A, Peter Yu Y, Zhou CY, Deng P, Park J, Zhang X, Lee J, Corpe M, Sharp K, Steward O, Eroglu C, Barres B, Zaucke F, Xu ZC, Luo ZD. Thrombospondin-4 contributes to spinal sensitization and neuropathic pain states. J Neurosci. 2012; 32:8977–8987. [PubMed: 22745497]

Knipper M, Zimmermann U, Rohbock K, Kopschall I, Zenner HP. Synaptophysin and GAP-43 proteins in efferent fibers of the inner ear during postnatal development. Brain Res Dev Brain Res. 1995; 89:73–86.

Kujawa SG, Liberman MC. Adding insult to injury: cochlear nerve degeneration after “temporary” noise-induced hearing loss. J Neurosci. 2009; 29:14077–14085. [PubMed: 19906956]

Kyriakides TR, Zhu YH, Smith LT, Bain SD, Yang Z, Lin MT, Danielson KG, Iozzo RV, LaMarca M, McKinney CE, Ginns EI, Bornstein P. Mice that lack thrombospondin 2 display connective tissue abnormalities that are associated with disordered collagen fibrillogenesis, an increased vascular density, and a bleeding diathesis. J Cell Biol. 1998; 140:419–430. [PubMed: 9442117]

Lawler J, Sunday M, Thibert V, Duquette M, George EL, Rayburn H, Hynes RO. Thrombospondin-1 is required for normal murine pulmonary homeostasis and its absence causes pneumonia. J Clin Invest. 1998; 101:982–992. [PubMed: 9486968]

Liauw J, Hoang S, Choi M, Eroglu C, Sun GH, Percy M, Wildman-Tobriner B, Bliss T, Guzman RG, Barres BA, Steinberg GK. Thrombospondins 1 and 2 are necessary for synaptic plasticity and functional recovery after stroke. J Cereb Blood Flow Metab. 2008; 28:1722–1732. [PubMed: 18594557]

Liberman LD, Wang H, Liberman MC. Opposing gradients of ribbon size and AMPA receptor expression underlie sensitivity differences among cochlear-nerve/hair-cell synapses. J Neurosci. 2011; 31:801–808. [PubMed: 21248103]

Liberman MC. Morphological differences among radial afferent fibers in the cat cochlea: an electron-microscopic study of serial sections. Hear Res. 1980; 3:45–63. [PubMed: 7400048]

Liberman MC. Single-neuron labeling in the cat auditory nerve. Science. 1982; 216:1239–1241. [PubMed: 7079757]

Liberman MC, Dodds LW, Pierce S. Afferent and efferent innervation of the cat cochlea: quantitative analysis with light and electron microscopy. J Comp Neurol. 1990; 301:443–460. [PubMed: 2262601]

Liu Q, Davis RL. Regional specification of threshold sensitivity and response time in CBA/CaJ mouse spiral ganglion neurons. J Neurophysiol. 2007; 98:2215–2222. [PubMed: 17715200]

Meyer AC, Frank T, Khimich D, Hoch G, Riedel D, Chapochnikov NM, Yarin YM, Harke B, Hell SW, Egner A, Moser T. Tuning of synapse number, structure and function in the cochlea. Nat Neurosci. 2009; 12:444–453. [PubMed: 19270686]

Mock B, Jones TA, Jones SM. Gravity receptor aging in the CBA/CaJ strain: a comparison to auditory aging. J Assoc Res Otolaryngol. 2011; 12:173–183. [PubMed: 21052761]

Moller, C. Balance disorders. In: Neton, VE., editor. Paediatric Audilogical Medicine. Whurr Publishers; London: 2002. p. 379-396.

Monzack EL, Cunningham LL. Lead roles for supporting actors: Critical functions of inner ear supporting cells. Hear Res. 2013

Muller M, von Hunerbein K, Hoidis S, Smolders JW. A physiological place-frequency map of the cochlea in the CBA/J mouse. Hear Res. 2005; 202:63–73. [PubMed: 15811700]

Naisbitt S, Kim E, Tu JC, Xiao B, Sala C, Valtschanoff J, Weinberg RJ, Worley PF, Sheng M. Shank, a novel family of postsynaptic density proteins that binds to the NMDA receptor/PSD-95/GKAP complex and cortactin. Neuron. 1999; 23:569–582. [PubMed: 10433268]

Nakanishi S. Metabotropic glutamate receptors: synaptic transmission, modulation, and plasticity. Neuron. 1994; 13:1031–1037. [PubMed: 7946343]

Nandi R, Luxon LM. Development and assessment of the vestibular system. Int J Audiol. 2008; 47:566–577. [PubMed: 18821226]

O'Shea KS, Liu LH, Kinnunen LH, Dixit VM. Role of the extracellular matrix protein thrombospondin in the early development of the mouse embryo. J Cell Biol. 1990; 111:2713–2723. [PubMed: 2277082]

Pirvola U, Arumae U, Moshnyakov M, Palgi J, Saarma M, Ylikoski J. Coordinated expression and function of neurotrophins and their receptors in the rat inner ear during target innervation. Hear Res. 1994; 75:131–144. [PubMed: 8071140]

Puel JL. Chemical synaptic transmission in the cochlea. Prog Neurobiol. 1995; 47:449–476. [PubMed: 8787031]

Raphael Y, Altschuler RA. Structure and innervation of the cochlea. Brain Res Bull. 2003; 60:397–422. [PubMed: 12787864]

Rio C, Dikkes P, Liberman MC, Corfas G. Glial fibrillary acidic protein expression and promoter activity in the inner ear of developing and adult mice. J Comp Neurol. 2002; 442:156–162. [PubMed: 11754168]

Risher WC, Eroglu C. Thrombospondins as key regulators of synaptogenesis in the central nervous system. Matrix Biol. 2012; 31:170–177. [PubMed: 22285841]

Rubel, EW. Ontogeny of structure and function in the vertebrate's auditory system. In: Jacobson, M., editor. Development of sensory systems. Springer; New York: 1978. p. 135-247.

Ruel J, Emery S, Nouvian R, Bersot T, Amilhon B, Van Rybroek JM, Rebillard G, Lenoir M, Eybalin M, Delprat B, Sivakumaran TA, Giros B, El Mestikawy S, Moser T, Smith RJ, Lesperance MM, Puel JL. Impairment of SLC17A8 encoding vesicular glutamate transporter-3, VGLUT3, underlies

nonsyndromic deafness DFNA25 and inner hair cell dysfunction in null mice. Am J Hum Genet. 2008; 83:278–292. [PubMed: 18674745]

Santarelli R. Information from cochlear potentials and genetic mutations helps localize the lesion site in auditory neuropathy. Genome Med. 2010; 2:91. [PubMed: 21176122]

Schmitz F, Konigstorfer A, Sudhof TC. RIBEYE, a component of synaptic ribbons: a protein's journey through evolution provides insight into synaptic ribbon function. Neuron. 2000; 28:857–872. [PubMed: 11163272]

Schwander M, Sczaniecka A, Grillet N, Bailey JS, Avenarius M, Najmabadi H, Steffy BM, Federe GC, Lagler EA, Banan R, Hice R, Grabowski-Boase L, Keithley EM, Ryan AF, Housley GD, Wiltshire T, Smith RJ, Tarantino LM, Muller U. A forward genetics screen in mice identifies recessive deafness traits and reveals that pejvakin is essential for outer hair cell function. J Neurosci. 2007; 27:2163–2175. [PubMed: 17329413]

Sendin G, Bulankina AV, Riedel D, Moser T. Maturation of ribbon synapses in hair cells is driven by thyroid hormone. J Neurosci. 2007; 27:3163–3173. [PubMed: 17376978]

Sobkowicz HM, Rose JE, Scott GE, Slapnick SM. Ribbon synapses in the developing intact and cultured organ of Corti in the mouse. J Neurosci. 1982; 2:942–957. [PubMed: 7097321]

Spoendlin H. Innervation patterns in the organ of Corti of the cat. Acta Otolaryngol. 1969; 67:239–254. [PubMed: 5374642]

Starr, A.; Zeng, F.; Michalewski, H.; Moser, T. Perspectives on auditory neuropathy: disorders of inner hair cell, auditory nerve, and their synapse. In: Basbaum, Al, et al., editors. The Senses: A Comprehensive Reference. Academic Press; New York: 2008. p. 397-412.

Sugawara M, Murtie JC, Stankovic KM, Liberman MC, Corfas G. Dynamic patterns of neurotrophin 3 expression in the postnatal mouse inner ear. J Comp Neurol. 2007; 501:30–37. [PubMed: 17206617]

Swinnen M, Vanhoutte D, Van Almen GC, Hamdani N, Schellings MW, D'Hooge J, Van der Velden J, Weaver MS, Sage EH, Bornstein P, Verheyen FK, VandenDriessche T, Chuah MK, Westermann D, Paulus WJ, Van de Werf F, Schroen B, Carmeliet P, Pinto YM, Heymans S. Absence of thrombospondin-2 causes age-related dilated cardiomyopathy. Circulation. 2009; 120:1585–1597. [PubMed: 19805649]

Taberner AM, Liberman MC. Response properties of single auditory nerve fibers in the mouse. J Neurophysiol. 2005; 93:557–569. [PubMed: 15456804]

Tanabe Y, Masu M, Ishii T, Shigemoto R, Nakanishi S. A family of metabotropic glutamate receptors. Neuron. 1992; 8:169–179. [PubMed: 1309649]

Tooney PA, Sakai T, Sakai K, Aeschlimann D, Mosher DF. Restricted localization of thrombospondin-2 protein during mouse embryogenesis: a comparison to thrombospondin-1. Matrix Biol. 1998; 17:131–143. [PubMed: 9694593]

Tran MD, Furones-Alonso O, Sanchez-Molano J, Bramlett HM. Trauma-induced expression of astrocytic thrombospondin-1 is regulated by P2 receptors coupled to protein kinase cascades. Neuroreport. 2012; 23:721–726. [PubMed: 22776902]

Tritsch NX, Bergles DE. Developmental regulation of spontaneous activity in the Mammalian cochlea. J Neurosci. 2010; 30:1539–1550. [PubMed: 20107081]

Tu JC, Xiao B, Naisbitt S, Yuan JP, Petralia RS, Brakeman P, Doan A, Aakalu VK, Lanahan AA, Sheng M, Worley PF. Coupling of mGluR/Homer and PSD-95 complexes by the Shank family of postsynaptic density proteins. Neuron. 1999; 23:583–592. [PubMed: 10433269]

Ullian EM, Sapperstein SK, Christopherson KS, Barres BA. Control of synapse number by glia. Science. 2001; 291:657–661. [PubMed: 11158678]

Wan G, Corfas G, Stone JS. Inner ear supporting cells: Rethinking the silent majority. Semin Cell Dev Biol. 2013

Xiao B, Tu JC, Petralia RS, Yuan JP, Doan A, Breder CD, Ruggiero A, Lanahan AA, Wenthold RJ, Worley PF. Homer regulates the association of group 1 metabotropic glutamate receptors with multivalent complexes of homer-related, synaptic proteins. Neuron. 1998; 21:707–716. [PubMed: 9808458]

Xiao B, Tu JC, Worley PF. Homer: a link between neural activity and glutamate receptor function. Curr Opin Neurobiol. 2000; 10:370–374. [PubMed: 10851183]

Xu J, Xiao N, Xia J. Thrombospondin 1 accelerates synaptogenesis in hippocampal neurons through neuroligin 1. Nat Neurosci. 2010; 13:22–24. [PubMed: 19915562]

Zuccotti A, Kuhn S, Johnson SL, Franz C, Singer W, Hecker D, Geisler HS, Kopschall I, Rohbock K, Gutsche K, Dlugaiczyk J, Schick B, Marcotti W, Ruttiger L, Schimmang T, Knipper M. Lack of brain-derived neurotrophic factor hampers inner hair cell synapse physiology, but protects against noise-induced hearing loss. J Neurosci. 2012; 32:8545–8553. [PubMed: 22723694]

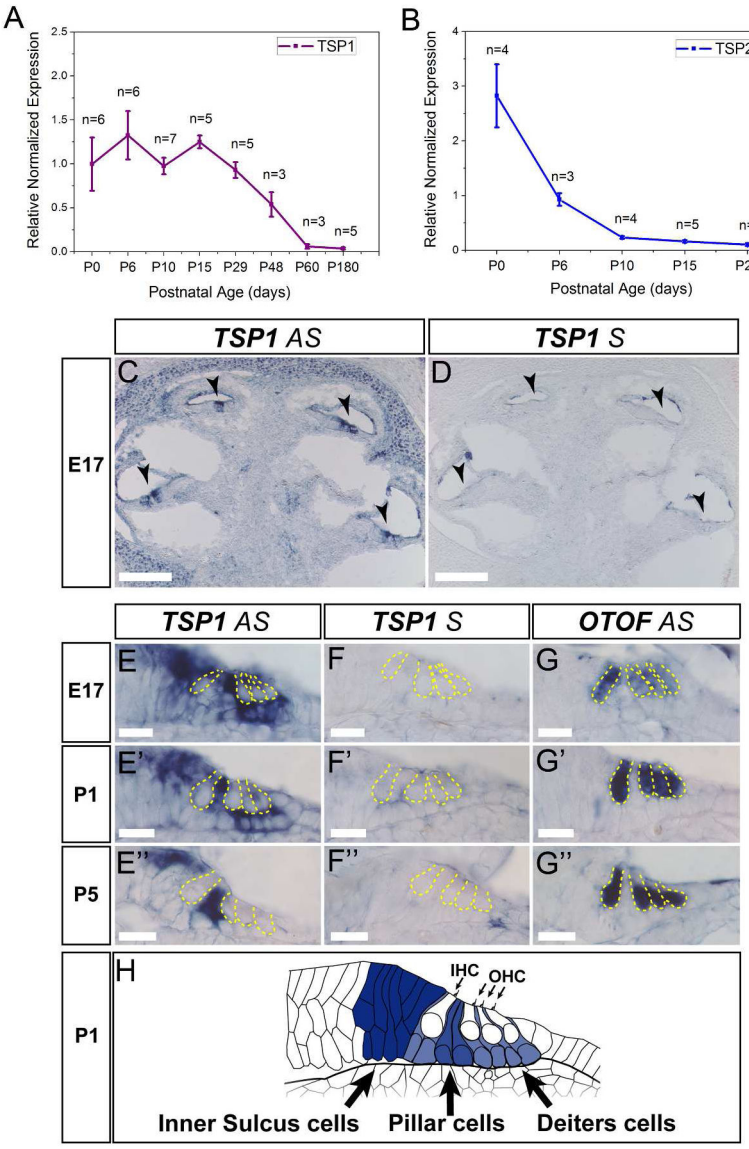

Figure 1.

Expression of TSP1 and TSP2 and in the mouse cochlea. ***A*** and ***B***, Quantitative RT-PCR was used to determine expression of TSP1 (***A***), TSP2 (***B***) genes in mouse cochlea at postnatal (P) day 0, 6, 10, 15, 29 for both genes, and additionally at P48, P60 and P120 for TSP1 gene. Data shown is the expression of the gene of interest relative to the internal standard, GAPDH. Results are expressed as mean ± standard error of the mean (SEM). ***C, D,*** *In situ* hybridization for TSP1 in cross-sections of E17 embryonic cochlea. Arrowheads indicate organ of Corti. ***E***, Close view of the organ of Corti with antisense (AS) TSP1 probe (***E***) at different developmental ages starting from E17 (***E***) and followed by P1 (***E′***) and P5 (***E″***). ***F***, Control sense (S) probe for TSP1 was included for all ages tested (***F*** – ***F″***) to confirm specificity. ***G***, AS otoferlin (OTOF) probe was used to visualize inner and outer hair cells in the organ of Corti at E17 (***G***), P1 (***G′***) and P5 (***G″***). Yellow dashed line indicates borders of IHC and OHC on ***E*** – ***G. H***, Schematic representation of the TSP1 expression at P1 with

strong expression in inner sulcus cells, phalangeal, pillar and Deiter's cells (expression pattern is shown as darker color for higher expression). AS – antisense probe, S – sense probe, P- postnatal day, IHC – inner hair cell, OHC – outer hair cell. Scale bar: C and D – 200 μm, E – G – 20 μm.

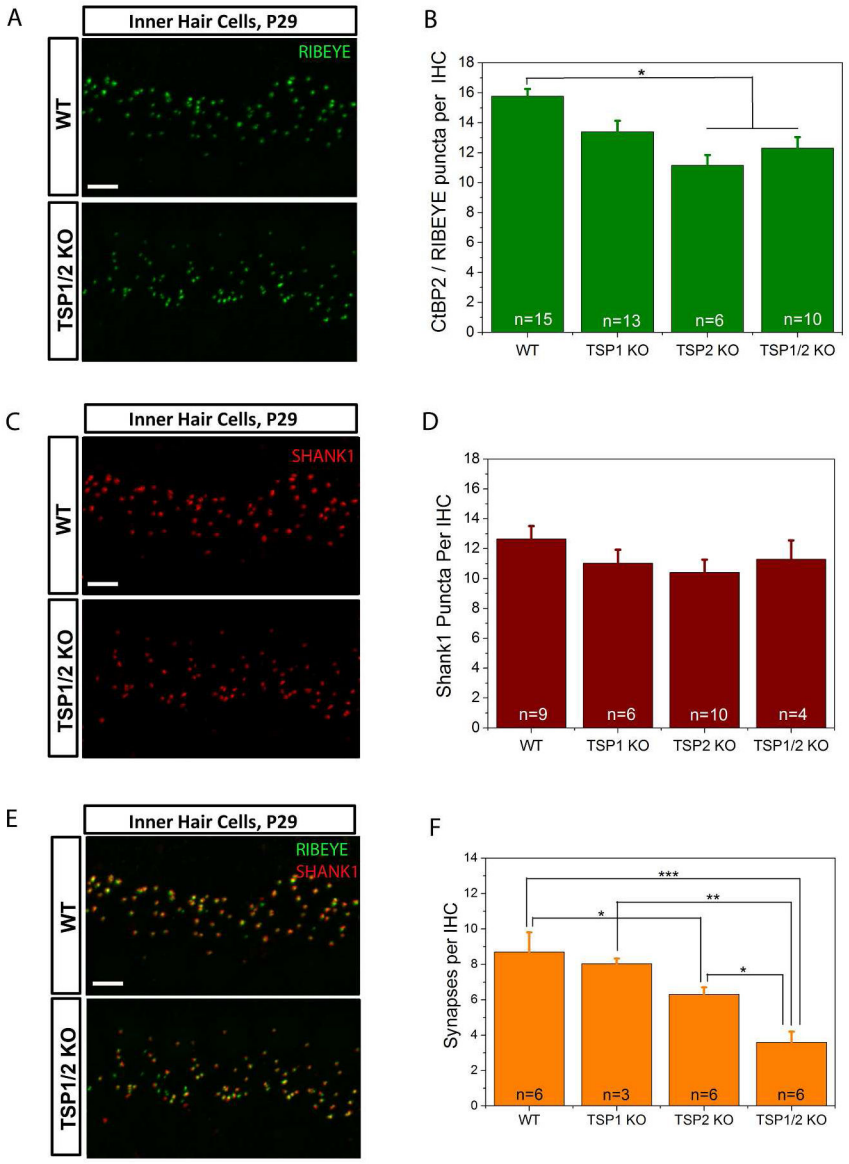

Figure 2.

Evaluation of synapse numbers in the TSP1, TSP2 and TSP1/2 mutants. ***A***, ***C***, and ***E***, Immunolabeling of RIBEYE (***A***), SHANK1 (***C***) or both (***E***) at IHC in WT and TSP1/2 mutants at 16 kHz region in the cochlea. Scale bar is 10 μm. ***P* values indicated are from Scheffe's post hoc test following a one-way ANOVA.** ***B***, Synaptic ribbon counts at 16 kHz region for TSP1, TSP2, TSP1/2 KOs and WT animals. **Significant differences were seen between WT and TSP2 KO (*P* = 0.002) and WT and TSP1/2 KO (*P* = 0.007).** ***D***, Quantification of the total number of postsynaptic marker SHANK1 showed no significant differences **(*P* = 0.201)** between WT and TSP mutants. ***F***, **Quantification of synapses. The average numbers of presynaptic RIBEYE that colocalized with postsynaptic SHANK1 per IHC were counted in WT and TSP mutant mice. A reduction in the number of synapses was observed in TSP1/2 KOs with respect to WT (*P* = 0.000), TSP1 KOs (*P* =**

0.002) and TSP2 KOs (*P* = 0.015). Synapse numbers were reduced in TSP2 KOs with respect to WT (*P* = 0.035). Number of animals tested (n) per genotype and type of staining is indicated on the graphs. Results are expressed as mean ± SEM. Significant differences are indicated by * for ***P* < 0.05, ** for *P* < 0.01 or *** for *P* < 0.001**.

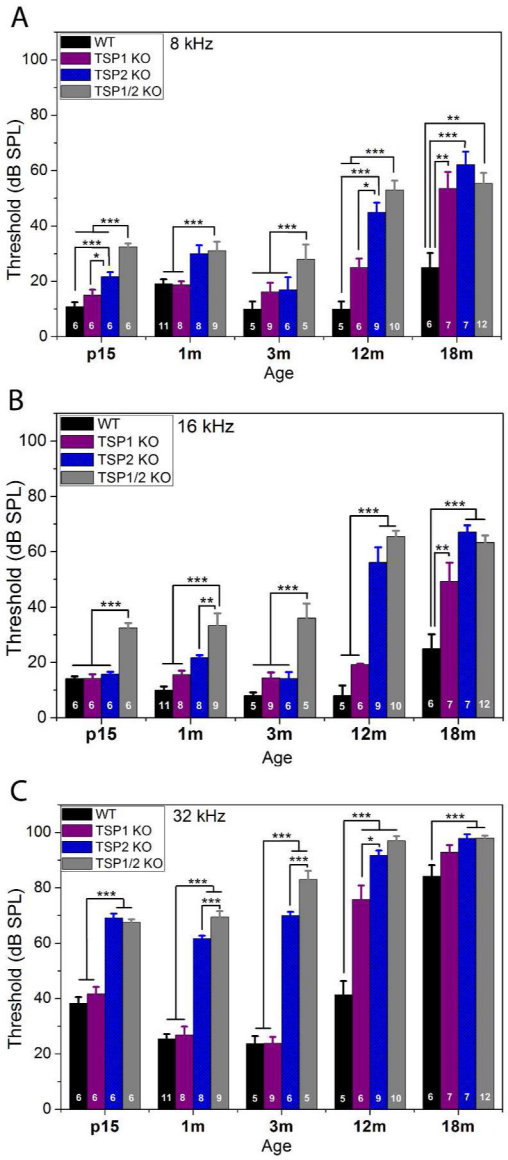

Figure 3.

Assessment of ABR thresholds in TSP mutant and WT mice at different ages. **Statistical analyses were performed using one- or two-way ANOVA followed by Scheffe's post hoc tests as appropriate.** At P15 TSP1 KOs had thresholds similar to WT mice. This pattern continued up to 12 months when TSP1 mutants developed a threshold shift at 32 kHz (***C***). TSP1 KOs developed threshold shifts at all frequencies (***A*** **–** ***C***) by 18 months of age. TSP2 mutants had elevated thresholds at 8 kHz (***A***) and 32 kHz (***C***), but not at 16 kHz (***B***). TSP2 KOs had similar thresholds to WT mice from 1 month to 12 months of age. At 12 months, TSP2 mutants developed threshold shifts at all frequencies. TSP1/2 KO had an elevation in threshold at all tested frequencies and at all ages tested. Number of animals tested for each genotype at each age is indicated on the respective bar on the graph. Scale bar in A, C and E is 5 μm. Thresholds presented as means ±SEM. Significant differences are indicated by *** for *P* < 0.05, ** for *P* < 0.01 or *** for *P* < 0.001.**

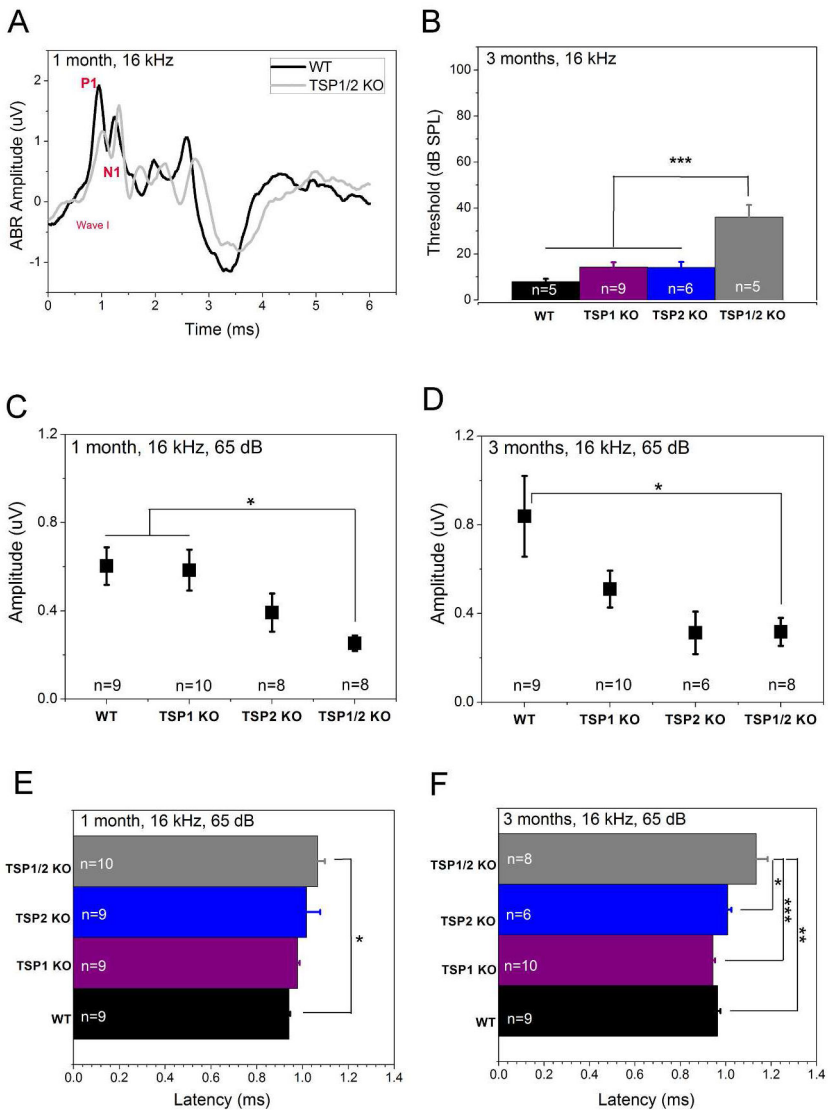

Figure 4.

Analysis of auditory nerve firing in TSP mutants at 1 month and 3 months of age. ABR wave I response amplitude and latency were analyzed at 65 dB for 16 kHz. **Statistical analyses were performed using a one-way ANOVA followed by Scheffe's post hoc test.** ***A***, Representative waveforms of WT (black line) and TSP1/2 mutants (grey line) at 1 month of age. Difference between P1 and N1 values indicate the amplitude of response. Distance time when stimulus was given (0 on the X axis) and time of response (P1 on the wave I) is the latency of the response. ***B***, ABR thresholds in WT and TSP mutant mice at 16 kHz indicate no significant threshold shift in TSP1 or TSP2 mutants as compared to WT. ***C***, ABR wave I amplitude was significantly reduced in TSP1/2 mutants as compared to WT at 1 month of age **(*P* = 0.026)**. ***B*** and ***D***, TSP1/2 KO had prolonged latency as compared to WT at 1 month **(*P* = 0.031)** (***B***) and 3 months **(*P* = 0.001)** (***D***) of age. ***C***, at 3 months of age, amplitude of wave I in TSP1/2 mutants was significantly reduced **(*P* = 0.038)**. Amplitude shift in TSP1 KOs was not significant. TSP2 mutants had an insignificant shift in amplitude

at this age. N-value near indicated genotype gives the number of animals that were used for the experiment. Quantification data is presented as mean ± SEM. Significant differences are indicated by *** for $P < 0.05$, ** for $P < 0.01$ or *** for $P < 0.001$.**

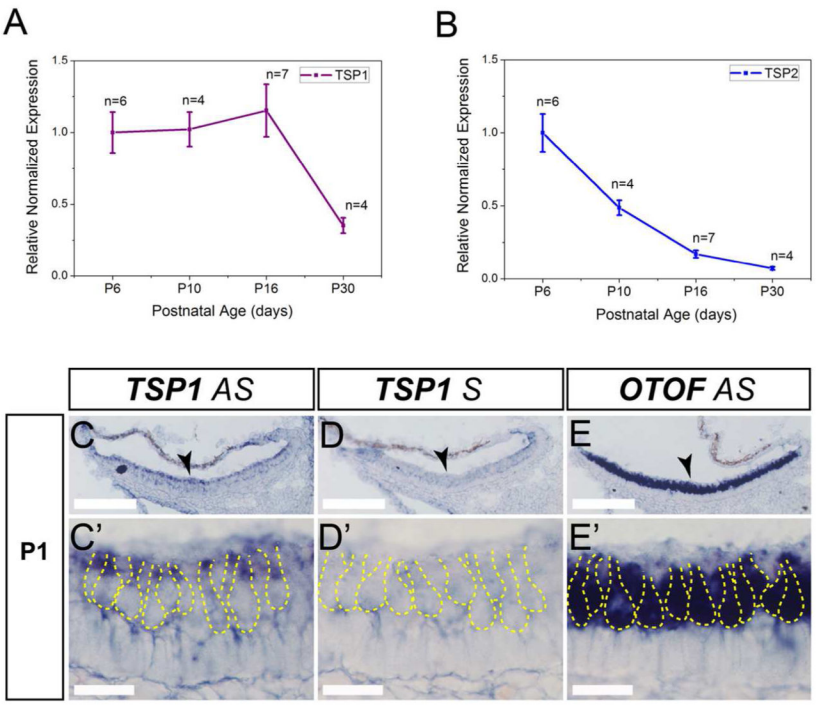

Figure 5.

Vestibular expression of TSP1 and TSP2. ***A, B***, Quantitative RT-PCR was used to determine expression of TSP1 (***A***) and TSP2 (***B***) genes from vestibular end organs at P6, P10, P16 and P30. Number of mice tested (n) for each age and genotype are indicated. Data shown is the expression of the gene of interest relative to the internal standard, GAPDH. Results are expressed as mean ± SEM. ***C***, ***D***, TSP1 anti-sense (AS, ***C***) and sense (S, ***E***) probes were used to localize gene expression in the neonatal utricle at P1. At higher magnification, TSP1 mRNA was detected in the cytoplasm of the hair cells (***C′***). No signal was observed with a sense probe for TSP1 shown as a negative control (***D′***). ***E***, *In situ* hybridization for otoferlin (OTOF) indicates the hair cells of P1 vestibular utricle. Dashed yellow line discriminates the hair cells from supporting cells. AS – antisense probe, S – sense probe, P - postnatal day. Scale bar in C – E is 200 μm, in C′ – E′ is 20 μm.

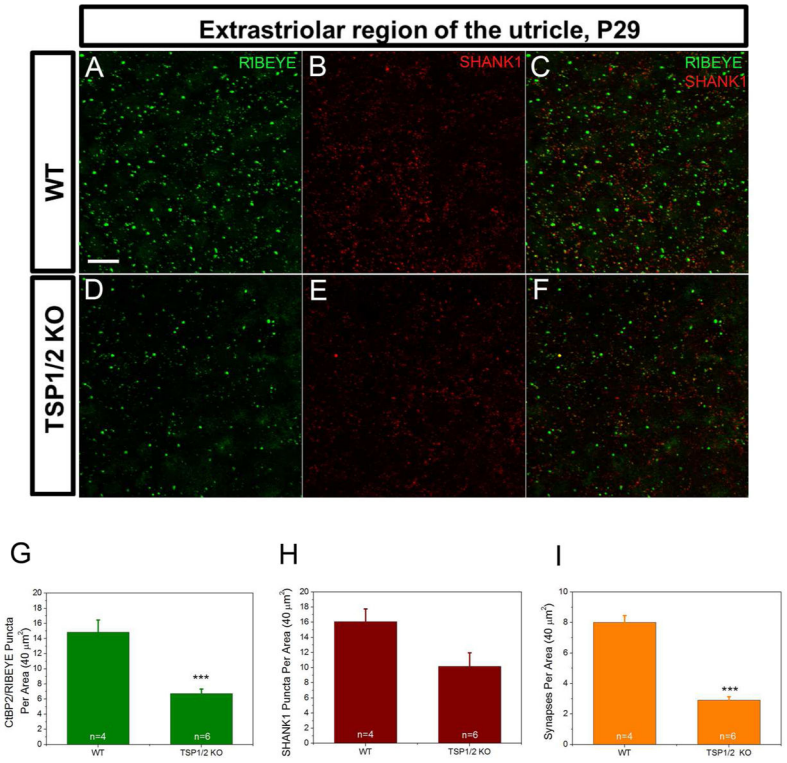

Figure 6.

Sensory epithelium of utricle stained with synaptic markers in WT and TSP1/2 mutants. **Counts were statistically analyzed with a one-way ANOVA followed by Scheffe's post hoc test.** ***A*** – ***C***, WT utricle stained with RIBEYE (***A***) and postsynaptic SHANK1 (***B***) at P29. Overlay view is shown in ***C.*** ***D*** – ***F***, TSP1/2 double mutant utricle stained with presynaptic ribbon marker RIBEYE (***D***) and postsynaptic SHANK1 (***E***). Colocalization of both markers is shown in ***F.*** ***G***, Synaptic ribbon counts per 40 µm^2 area of utricle in TSP1/2 KOs and WT animals. Ribbon numbers in TSP1/2 mutants were lower than WT **(*P* = 0.001)**. ***H***, Quantification of the postsynaptic marker SHANK1. No significant difference was observed between WT and TSP1/2 mutants. ***I***, Average number of synapses determined by presynaptic RIBEYE that colocalized with postsynaptic SHANK1 per 40 µm^2 in WT and TSP1/2 mutant mice. Number of synapses was reduced in TSP1/2 mutants compared to WT **(*P* = 0.000)**. Number of animals tested (n) per genotype and type of staining are indicated on the graphs. Scale bar in A is 10 µm and applies to B – F. Results are expressed as mean ± SEM. Significant differences are indicated by *** for *P* < 0.05, ** for *P* < 0.01 or *** for *P* < 0.001.**

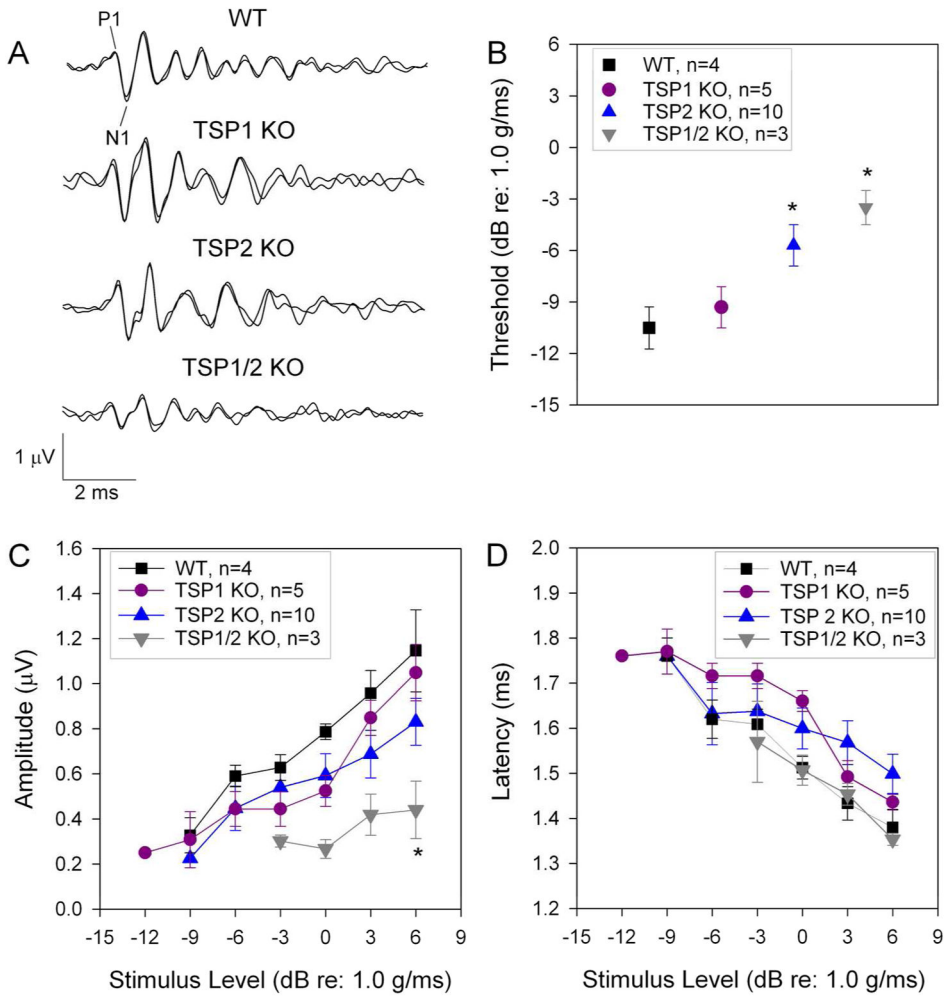

Figure 7.

Contribution of TSP1 and TSP2 to vestibular function. ***A***, Representative VsEP waveforms collected at +6 dB (re: 1.0 g/ms) for the four genotypes tested. P1 - N1 represents the first response peak measured for latency and amplitude. **A one-way ANOVA followed by post hoc test was used for statistical analysis.** ***B***, On average, VsEP thresholds were significantly elevated in TSP1/2 KO mice (downward triangle) compared to WT (square) **(*P* = 0.010)** and TSP1 KO (circle) mice **(*P* = 0.023)**. TSP2 KO mice (upward triangle) also had VsEP thresholds significantly higher than WT mice **(*P* = 0.020)**. ***C***, VsEP wave I amplitudes were significantly reduced for TSP1/2 KO mice compared to WT **(*P* = 0.011)** and TSP1 KO mice **(*P* = 0.014)**. ***D***, VsEP wave I latencies were not significantly different across genotypes. Significant differences are indicated by *** for *P* < 0.05, ** for *P* < 0.01 or *** for *P* < 0.001.**